Maximum-Density Droplet and Charge Redistributions in Quantum Dots at High Magnetic Fields

T. H. Oosterkamp,[1] J. W. Janssen,[1] L. P. Kouwenhoven,[1] D. G. Austing,[2] T. Honda,[2] and S. Tarucha[2,3]
[1]*Department of Applied Physics and DIMES, Delft University of Technology, P.O. Box 5046, 2600 GA Delft, The Netherlands*
[2]*NTT Basic Research Laboratories, 3-1, Morinosoto, Wakamiya, Atsugi-shi, Kanagawa 243-01 Japan*
[3]*Tokyo University, 7-22-1 Roppongi, Minato-ku, Tokyo 106, Japan*
(Received 28 September 1998)

We have measured electron transport through a vertical quantum dot containing a tunable number (between 0 and 40) of electrons. Over a region of the magnetic field the electrons are spin polarized and occupy successive angular momentum states. This is the maximum-density-droplet (MDD) state. The stability region where the MDD is the ground state decreases for increasing electron number. The instability of the MDD and other transitions in this high B region are accompanied by a redistribution of charge which abruptly changes the area of the electron droplet. [S0031-9007(99)08873-0]

PACS numbers: 73.20.Dx, 71.45.Gm, 73.40.Hm

In this Letter we study quantum dots [1,2] in the quantum Hall regime and exploit the fact that dots contain a tunable and well-defined number of electrons. In particular, we consider the spin-polarized, maximum-density-droplet (MDD) state at high magnetic fields that corresponds to filling factor $\nu = 1$ in a large two dimensional electron gas. The stability of this state is set by a balance of forces [3–6] acting on this finite electron system, namely, the inward force of the confining potential, the repulsive force of the direct Coulomb interaction between electrons, and a binding force due to the exchange interaction. In addition, Zeeman energy and correlation effects are important. As the magnetic field and the electron number are changed, the relative strengths of these forces are tuned, which induces transitions between the MDD and other states. Earlier these transitions were measured in the linear response regime [1,7]. We report detailed measurements in linear and nonlinear transport showing that the transitions are accompanied by a significant *redistribution of charge* in this many-body system.

Our vertical quantum dot is made from a double barrier resonant tunneling structure with an InGaAs well, AlGaAs barriers, and n-doped GaAs source and drain contacts [8]. The device is processed in the shape of a submicron circular pillar with a diameter of 0.54 μm, and a self-aligned gate surrounds it. We discuss data taken on one particular device, but comparable results have been obtained on several devices. A magnetic field, B, is applied perpendicular to the plane in which the electrons are confined. The energy spectrum of the quantum dot is derived from transport experiments at a temperature of 100 mK in the Coulomb blockade regime. A dc source-drain voltage, V_{SD}, is applied and the current, I, is measured versus gate voltage, V_g. The electron number, N, varies from about 40 at $V_g = 0$ to $N = 0$ at the pinch-off voltage, $V_g \approx -2$ V.

Figure 1 shows the Coulomb current peaks versus B for $N = 0$ to 18. On increasing V_g, current peaks are measured for every extra electron that enters the dot. Figure 1 consists of many such current traces that have been offset horizontally by a value corresponding to B. The peaks are seen to evolve in pairs for $B < 2$ T, implying that each single-particle state is filled with two electrons of opposite spin [9]. Kinks indicate crossings between single-particle states. The dotted line marks the evolution of the B value at which all electrons occupy spin-degenerate states belonging to the lowest orbital Landau level (i.e., this corresponds to $\nu = 2$ in a 2DEG). As B is increased further it becomes energetically favorable for an electron to flip its spin and move to the edge of the dot (see left diagram above Fig. 1). These spin-flip processes have been studied in detail both experimentally [7,10] and theoretically [3,4].

After the last spin flip (filled circles in Fig. 1) all electrons are spin polarized (i.e., the total spin $S = N/2$ and the filling factor $\nu = 1$). Here, the N electrons occupy successive angular momentum states and the total angular momentum $M = \frac{1}{2}N(N-1)$. This is the densest, spin-polarized electron configuration allowed by the available quantum states and is therefore referred to as the maximum density droplet [5]. Its observation was reviewed in Ref. [1]. For $N = 2$ the spin flip corresponds to a singlet ($S = 0$) to triplet ($S = 1$) transition where simultaneously M changes from 0 to 1 [11]. Also, the transitions in the $N = 3$ to 6 traces have been identified as increases in S and M until the MDD is reached at the solid circle in Fig. 1 [12]. For larger N the beginning of the MDD first moves to larger B and then becomes roughly independent of N.

When B is increased further, the angular momentum states shrink in size such that the density of the MDD increases. We have pictured this in the right diagram above Fig. 1 as an electron droplet that does not spread out over the full available area of the confining potential. At some threshold B value (open circles) the direct Coulomb interaction has become so large that the MDD breaks apart into a larger, lower density droplet (LDD). Assuming that the droplet remains spin polarized ($S = N/2$), this

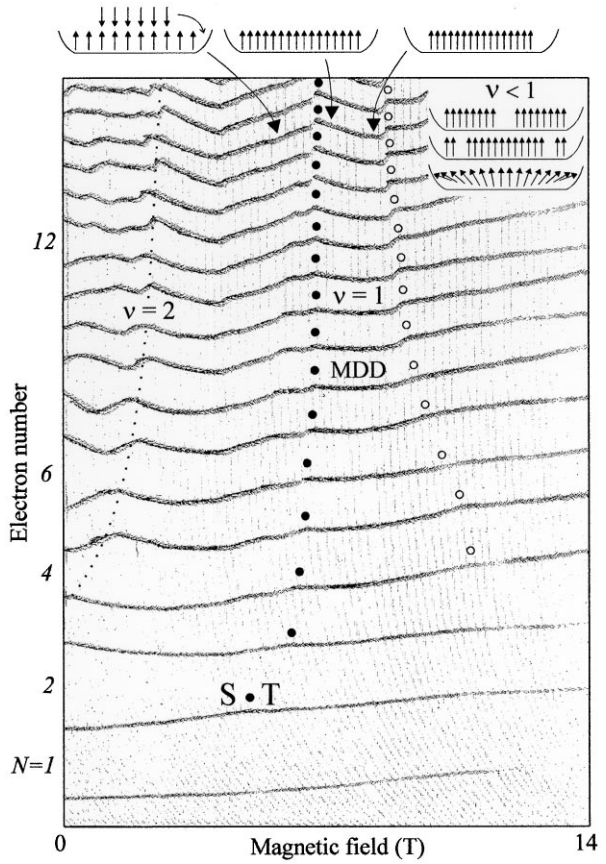

FIG. 1. Magnetic field evolution of the Coulomb blockade peaks for the first 18 electrons ($V_{SD} = 100\ \mu$V). The figure is built up of many current traces versus V_g (from -2.1 to -0.8 V) that have been offset by a value proportional to B. The solid (open) dots mark the beginning (end) of the MDD, which for $N = 2$ is the singlet-triplet transition. The dotted line indicates filling factor $\nu = 2$. Top: Schematic diagrams of the spin-flip processes (left) and of the MDD at two B fields (middle and right). Inset: Schematic diagrams of three possible lower density droplet (LDD) states, with a hole in the center of the dot, at the edge, or a spin texture.

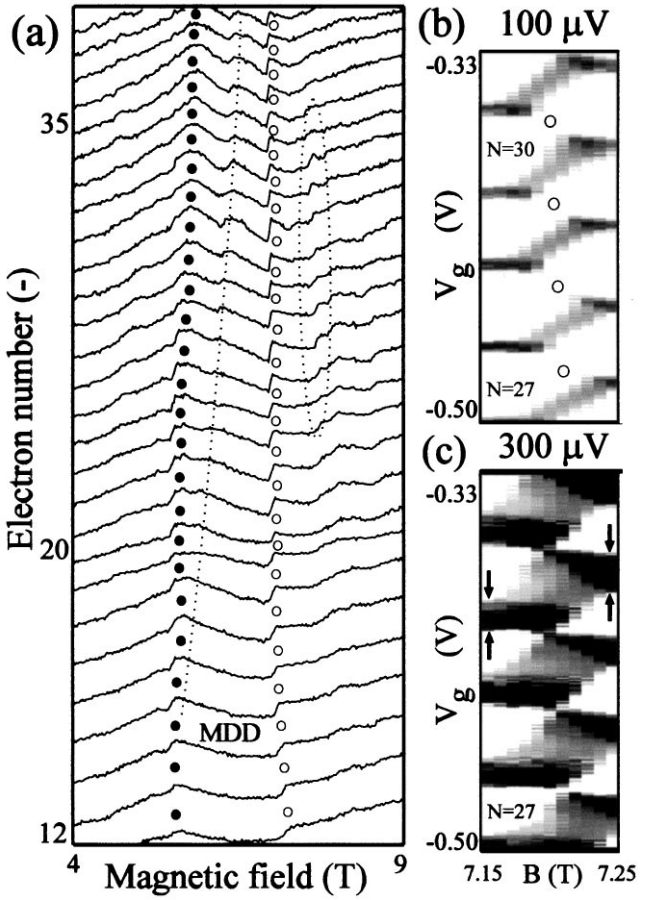

FIG. 2. (a) Peak positions versus B for $N = 12$ to 39 extracted from a data set as in Fig. 1 (V_g is swept from -0.9 to -0.1 V). Open and closed circles mark the same transitions as in Fig. 1. Dotted lines indicate additional transitions. (b) and (c): Grey scale plots of the current versus V_g for B values in a small interval around the step marked by the open circles. $V_{SD} = 100\ \mu$V in (b) and 300 μV in (c). The arrows in (c) highlight that the peak width after the step is larger than before the step.

implies that no longer are all successive angular momentum states occupied and that $M > \frac{1}{2}N(N-1)$. Whether the unoccupied angular momentum states are located in the center [5] or at the edge [13] (see inset of Fig. 1) depends on the relative strengths of the confinement, exchange, and direct Coulomb interactions, as well as the Zeeman energy and correlation effects. It has been suggested, especially when the Zeeman energy is small, that the MDD may become unstable towards the formation of a spin texture [14]. The stability conditions for the MDD state (i.e., the B range between solid and open circles) have been calculated in several different theoretical approaches [4–6]. It is difficult to make a quantitative comparison with our data, since the calculated phase diagrams are very sensitive to the finite thickness of the quantum dot and to screening effects from electrons in the source and drain contacts.

Figure 2(a) shows the peak positions versus B for larger N. Within the boundaries of solid and open circles a new transition seems to develop for $N > 15$. This indicates a new electronic configuration that develops inside the region between the solid and open circles (see dotted line). We believe the MDD continues on the right of this transition but, since we cannot identify the new state on the left of it, this is not indisputable. At this moment no calculations exist for our specific sample parameters.

Note that the kinks in the peak evolution that mark the boundaries of the MDD for small N turn into abrupt steps for $N \gtrsim 10$. Also the new transition between the solid and open circles becomes a step as N is increased, and at higher B (marked with the dotted oval) additional steps can be discerned in Fig. 2(a). We now argue that at all these steps, the *charge distribution* of the droplet changes abruptly.

Figures 2(b) and 2(c) show the current versus V_g ($N =$ 27 to 31) in grey scale for B values around the steps at the open dots. The step width is about 50 mT. For $V_{SD} =$ 100 μV the peaks are much narrower than their spacings. An increased source-drain voltage $V_{SD} = 300\ \mu$V

broadens the peaks. The important point is that the peak width, ΔV_g, increases by about 10% after crossing the step as indicated by the arrows. At low temperature $\alpha \Delta V_g = eV_{\mathrm{SD}}$, where the α factor is roughly proportional to the inverse of the area of the droplet [15]. The change in peak width implies that the dot area changes abruptly by about 10%.

It is clearly seen in Fig. 2(c) that the peak width *during* the step is about twice the width outside the step region. All steps show this behavior. To study the nature of these unusual steps we have measured the excitation spectra. Figure 3 presents detailed dI/dV_{SD} traces in the V_{SD}-V_g plane for ten B values [16] around a particular step that separates two different LDD states in the magnetic field regime marked by the dotted oval in Fig. 2(a). We stress that the same behavior is found at all steps. At the lowest and highest magnetic fields the Coulomb blockade regions have the expected diamond shape. The diamonds at $B = 7.48$ T are about 10% smaller in the V_{SD} direction, indicating that the necessary energy to overcome Coulomb blockade has decreased by $\sim$10%. This is again consistent with a $\sim$10% larger dot area after the charge redistribution. A striking observation is that the shapes of the diamonds measured for B values inside the step region are severely distorted. The size of the Coulomb blockade region collapses here to as little as $\sim$40% of its value outside the step region. This agrees with the peak broadening by about a factor of 2 during the steps in Fig. 2(c). We are not aware of such a collapse of the Coulomb gap in any study of metallic or semiconducting Coulomb blockade systems.

Distorted and collapsing Coulomb blockade regions can be obtained within a simple phenomenological model [17]. In the standard model for Coulomb blockade the total energy $U_N^{\gamma}(V_g)$ for a charge configuration γ is described by a set of parabolas [solid parabolas in Fig. 4(a)]. A tunnel event from N to $N + 1$ is possible above a threshold voltage that depends linearly on V_g [solid lines and hatched regions in Fig. 4(b)]. At crossings between adjacent parabolas this threshold voltage vanishes. The precise value of V_g where the crossing between the Nth and $(N + 1)$th parabolas occurs depends on the "offset charge" of the charge state γ [15]. The total energy $U_N^{\delta}(V_g)$ for a charge configuration δ is also described by parabolas [dashed parabolas in Fig. 4(a)]. However, the offset charge for state δ can differ from that of state γ when they have different charge distributions; i.e., the two sets of parabolas are shifted horizontally. We note that usually the offset charges of different states are assumed to be equal. When B is changed, the two sets of parabolas become comparable in energy [Fig. 4(c)], such that at a particular V_g value (open dots) the ground state of the N-electron system changes from γ to δ. This, and the fact that tunnel events can occur between different charge distributions, e.g., from U_N^{δ} to U_{N+1}^{γ}, leads to more complex shapes of the Coulomb blockade regions [see Figs. 4(c) and 4(d)]. To make a detailed comparison with this model we have replotted one data set from Fig. 3 in Fig. 4(f), together with a schematic representation of its main features [Fig. 4(e)]. Three types of features can be distinguished in Fig. 4(e), which correspond to tunnel events between two solid parabolas (from U_N^{γ} to U_{N+1}^{γ}), between two dashed parabolas (from U_N^{δ} to U_{N+1}^{δ}), or between a dashed and a solid parabola (from U_N^{δ} to U_{N+1}^{γ}). The first two types of tunnel events lead to features having the same slopes as the regular diamonds at the lowest and highest B fields in Fig. 3 and are marked by solid and dashed lines in Fig. 4(e). The third feature [marked by thin lines in Fig. 4(e)] has a slope that is much smaller since here the centers of the parabolas corresponding to N and $N + 1$

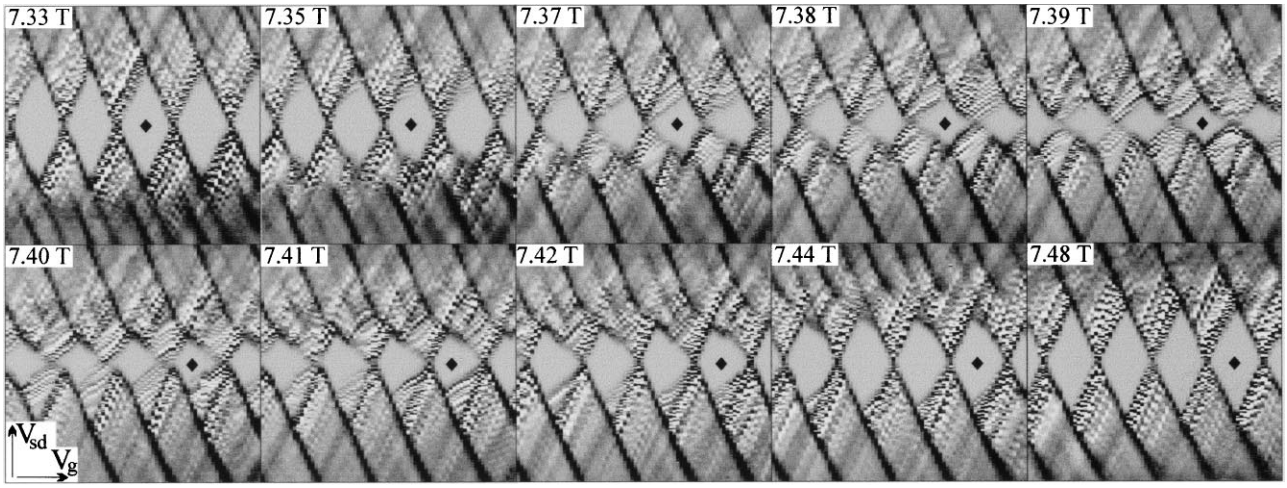

FIG. 3. Grey scale plots of dI/dV_{SD} in the V_g-V_{SD} plane for ten B values before, during, and after a particular step corresponding to different charge distributions ($-1 < V_{\mathrm{SD}} < +1$ mV and $-0.42 < V_g < -0.32$ V). $N = 31$ is marked by a solid diamond. The Coulomb blockade regions at the lowest and highest B field have the familiar diamond shapes. In between, the Coulomb blockade regions are severely distorted. Excited state transitions are visible as dark lines [18]. As B is changed these evolve into the edges of the regular Coulomb blockade diamonds at the lowest and highest B field.

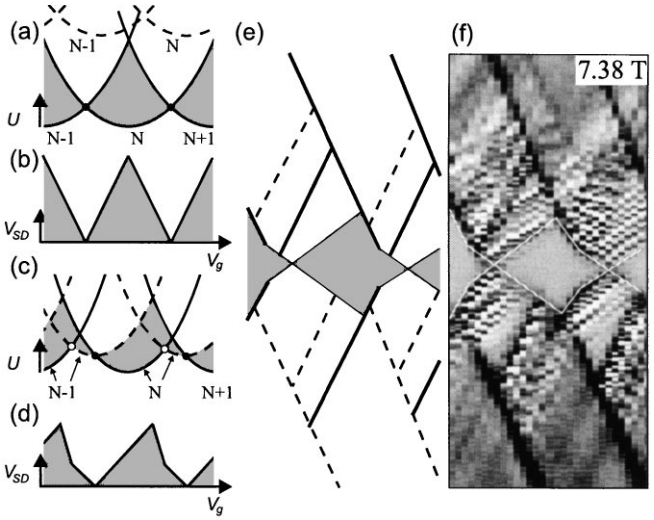

FIG. 4. (a) Total energy $U(V_g)$ for two different charge distributions (solid and dashed curves, respectively). The three parabolas correspond to $N-1$, N, and $N+1$ electrons. Current flows when transitions can occur between parabolas of consecutive electron numbers. At low V_{SD} such transitions occur at the solid dots. In between two solid dots, the minimum V_{SD} for current is proportional to the difference in energy between the two parabolas (grey regions). (b) Transition diagram in terms of V_g and V_{SD} (i.e., half Coulomb diamonds) corresponding to the situation in (a). (c) Same as in (a) but at larger B. Now the dashed parabolas are comparable in energy to the solid parabolas which gives a transition of the N-electron system from one charge distribution to another as V_g is varied (open dots). This leads to a different shape of the Coulomb blockade region shown in (d). The transition diagram in (e) shows transitions between two solid (dashed) parabolas as solid (dashed) lines, and those between solid and dashed parabolas as thin lines. In Fig. 3 the solid (dashed) lines become clearer as B is decreased (increased) and finally become the boundaries of the ordinary diamond-shaped Coulomb blockade regions at 7.33 T (7.48 T). (f) dI/dV_{SD}-data around $N = 31$ taken from Fig. 3 at 7.38 T. The edge of the Coulomb blockade regions have been emphasized with a white line.

electrons are much closer together. Note that in this case [and also during the steps in Figs. 2(b) and 2(c)] the current is 2 to 3 times smaller than when tunneling occurs between two states with the same charge distribution. This implies that tunneling between two different charge distributions has a reduced probability. A detailed comparison of the data in Fig. 3 with this phenomenological model shows that the development of the Coulomb blockade regions as well as the excited state resonances observed in Fig. 3 is consistent with a gradual change in the relative displacement of the two sets of parabolas. From this we again conclude that the instability of the MDD and of other states in this magnetic field regime is accompanied by a redistribution of charge. It remains a challenge, however, to calculate the microscopic origin of the difference in offset charge between two states with a different charge distribution. Then the effect of the gate voltage on the total energy $U_N^{\gamma}(V_g)$ and the effect of screening from the leads has to be taken into account microscopically.

We thank G. Bauer, S. Cronenwett, M. Danoesastro, M. Devoret, L. Glazman, R. van der Hage, J. Mooij, Yu. Nazarov, and S. J. Tans for experimental help and discussions. The work was supported by the Dutch Foundation for Fundamental Research on Matter (FOM), and by the NEDO joint research program (NTDP-98).

[1] R. Ashoori, Nature (London) **379**, 413 (1996).
[2] L. P. Kouwenhoven and C. M. Marcus, Phys. World **11**, 35 (1998).
[3] A. K. Evans et al., Phys. Rev. B **48**, 11 120 (1993); J. H. Oakin *et al.*, Phys. Rev. B **49**, 5718 (1994); J. J. Palacios *et al.*, Phys. Rev. B **50**, 5760 (1994); T. H. Stoof and G. E. W. Bauer, Phys. Rev. B **52**, 12 143 (1995); A. Wojs and P. Hawrylak, Phys. Rev. B **56**, 13 227 (1997).
[4] M. Ferconi and G. Vignale, Phys. Rev. B **50**, 14 722 (1994); S. R.-E. Yang *et al.*, Phys. Rev. Lett. **71**, 3194 (1993); M. Ferconi and G. Vignale, Phys. Rev. B **56**, 12 108 (1997); S. M. Reimann *et al.* (to be published).
[5] A. H. MacDonald *et al.*, Aust. J. Phys. **46**, 345 (1993).
[6] P. A. Maksym and T. Chakraborty, Phys. Rev. Lett. **65**, 108 (1990); P. A. Maksym *et al.*, Physica (Amsterdam) **212B**, 213 (1995); J. H. Oaknin *et al.*, Phys. Rev. Lett. **74**, 5120 (1995); Kang-Hun Ahn *et al.*, Phys. Rev. B **52**, 13 757 (1995); M. Eto, Jpn. J. Appl. Phys. **38**, 376 (1999); A. Harju *et al.*, Europhys. Lett. **41**, 407 (1998).
[7] O. Klein *et al.*, Phys. Rev. Lett. **74**, 785 (1995); Phys. Rev. B **53**, R4221 (1996).
[8] D. G. Austing *et al.*, Jpn. J. Appl. Phys. **34**, 1320 (1995); Semicond. Sci. Technol. **11**, 388 (1996).
[9] S. Tarucha *et al.*, Phys. Rev. Lett. **77**, 3613 (1996).
[10] P. L McEuen *et al.*, Phys. Rev. B **45**, 11 419 (1992); N. C. van der Vaart *et al.*, Phys. Rev. Lett. **73**, 320 (1994); D. G. Austing *et al.*, Jpn. J. Appl. Phys. **38**, 372 (1999); P. Hawrylak *et al.*, Phys. Rev. B **59**, 2801 (1999).
[11] M. Wagner *et al.*, Phys. Rev. B **45**, 1951 (1992).
[12] L. P. Kouwenhoven *et al.*, Science **278**, 1788 (1997).
[13] C. de C. Chamon and X. G. Wen, Phys. Rev. B **49**, 8227 (1994).
[14] A. Karlhede *et al.*, Phys. Rev. Lett. **77**, 2061 (1996); J. H. Oaknin *et al.*, Phys. Rev. B **54**, 16 850 (1996).
[15] For a review on quantum dots see L. P. Kouwenhoven *et al.*, in *Mesoscopic Electron Transport*, edited by L. Sohn *et al.*, NATO ASI, Ser. E (Kluwer, Dordrecht, 1997). See also http://vortex.tn.tudelft.nl/~leok/papers/. In a capacitance model $\alpha = eC_g/C_{\Sigma}$. The total capacitance C_{Σ} is in our geometry roughly proportional to the dot area, and the gate capacitance C_g increases slowly with the dot area. However, it is not clear how well an MDD state can be modeled by capacitances.
[16] An animation of the data in Fig. 3 can be found at http://vortex.tn.tudelft.nl/research/dots/mdd.html
[17] S. J. Tans *et al.*, Nature (London) **394**, 761 (1998).
[18] Because of the slight asymmetry between the barriers the excited state resonances lines in Fig. 3 are most pronounced when they run from the bottom right to the top left.